https://doi.org/10.5194/egusphere-2024-74
Preprint. Discussion started: 5 February 2024

Different Formation Pathways of Nitrogen-containing Organic Compounds in Aerosols and Fog Water in Northern China

Wei Sun[1, 2], Xiaodong Hu[3], Yuzhen Fu[4], Guohua Zhang[1, 2] *, Yujiao Zhu[5], Xinfeng Wang[5], Caiqing Yan[5], Likun Xue[5], He Meng[6], Bin Jiang[1, 2], Yuhong Liao[1, 2], Xinming Wang[1 ,2], Ping'an Peng[1, 2], and Xinhui Bi[1 ,2]*

[1] State Key Laboratory of Organic Geochemistry and Guangdong Key Laboratory of Environmental Protection and Resources Utilization, Guangzhou Institute of Geochemistry, Chinese Academy of Sciences, Guangzhou, 510640, PR China
[2] Guangdong-Hong Kong-Macao Joint Laboratory for Environmental Pollution and Control, Guangzhou Institute of Geochemistry, Chinese Academy of Sciences, Guangzhou 510640, PR China
[3] Jiangmen Laboratory of Carbon Science and Technology, Hong Kong University of Science and Technology (Guangzhou), Jiangmen 529199, PR China
[4] Hainan Research Academy of Environmental Sciences, Haikou 571126, PR China
[5] Environment Research Institute, Shandong University, Qingdao 266237, PR China
[6] Qingdao Eco-environment Monitoring Center of Shandong Province, Qingdao 266003, PR China

Correspondence to: Bi X.H. (bixh@gig.ac.cn); Zhang G.H. (zhanggh@gig.ac.cn)

Abstract. While aqueous-phase processing contributes to the formation of nitrogen-containing organic compounds (NOCs), the detailed pathways are not well understood. In this study, the molecular composition of NOCs in both pre-fog aerosols and fog water collected at a suburban site in northern China was characterized using Fourier-transform ion cyclotron resonance mass spectrometry in both negative and positive modes of electrospray ionization (ESI- and ESI+). In both pre-fog aerosols and fog water, NOCs account for number fractions of more than 60% in all assigned formulas in ESI- mode and more than 80% in ESI+ mode. By comparing the molecular composition of biomass burning, coal combustion, and vehicle emissions, 72.3% of NOCs in pre-fog aerosols were assigned as originating from these primary anthropogenic sources (pNOCs), while the remaining NOCs were regarded as secondary NOCs formed in aerosol (saNOCs). On the other hand, the unique NOCs in fog water were regarded as secondary NOCs formed in fog (sfNOCs). According to "precursor-product pair" screening involving 39 reaction pathways, we found that the nitration reaction, the amine pathway and the intramolecular N-heterocycle pathway of NH_3 addition reactions contribute to 43.6%, 22.1%, and 11.6% of saNOCs, but 26.8%, 28.4%, and 29.7% of sfNOCs, respectively. Such distinct formation pathways are most likely attributed to the diverse precursors and the aqueous acidity. Correspondingly, saNOCs contain more abundant carbohydrates-like and highly oxygenated compounds with two nitrogen atoms compared to pNOCs, whereas sfNOCs contain more lipids-like with fewer oxygen atoms. The results reveal the disparity in secondary processes that contribute to the richness of NOCs in aerosols and fog water. The findings are valuable for understanding the formation and control of organic nitrogen pollution.

https://doi.org/10.5194/egusphere-2024-74
Preprint. Discussion started: 5 February 2024

1 Introduction

Nitrogen-containing organic compounds (NOCs), which mainly includes organonitrates, amines, amino acids, nitroaromatics, and nitrogen-heterocyclic compounds, have been widely detected in aerosols, cloud/fog water, and rain water (Altieri et al., 2012; Li et al., 2020c; Wang et al., 2018; Feng et al., 2016; Leclair et al., 2012; Ditto et al., 2022). As essential contributors to the absorption of brown carbon, NOCs significantly influence the radiative balance (Yang et al., 2022; Jimenez et al., 2022; Jiang et al., 2021; Huang et al., 2020). Some NOCs, e.g., nitroaromatics, are considered as phytotoxins and suspected carcinogens (Harrison et al., 2005). Thus, an in-depth study of the characteristics, sources, and atmospheric processes of NOCs is crucial for comprehending their climate and health effects.

Both primary emissions and secondary formation contribute to NOCs in the atmosphere. Benefiting from ultra-high Fourier-transform ion cyclotron resonance mass spectrometry (FT-ICR MS), thousands of NOCs molecules have been detected in primary anthropogenic sources, including biomass burning (BB), coal combustion (CC), and vehicle emission (VE) smoke (Tang et al., 2020; Song et al., 2019; Song et al., 2018; Song et al., 2021). Meanwhile, the aqueous-phase reactions have been identified as important pathways for the formation of secondary NOCs. Recent studies have observed a positive relationship between NOCs and relative humidity or aerosol liquid water (Liu et al., 2023a; Cai et al., 2023; Jiang et al., 2023) as well as the abundant NOCs in cloud/fog water (Kim et al., 2019; Boone et al., 2015). Laboratory studies have indicated two major pathways of NOCs formation in the aqueous phase: 1) the organic precursors can be nitrated by NO_2 radical or nitronium ion (NO_2^+) and form NOCs, e.g., nitroaromatics (Kroflic et al., 2015; Vione et al., 2005); and 2) the reaction of carbonyl compounds (e.g., glyoxal and methylglyoxal) with ammonium and/or amine in the aqueous phase, known as Maillard reactions, leads to the formation of reduced NOCs, e.g., imidazoles (Jimenez et al., 2022; De Haan et al., 2009; Kua et al., 2011; De Haan et al., 2018). The formations of both nitration and Maillard products, such as dinitrophenols, methylnitrocatechols, and imidazoles, have been observed in aerosol liquid water or cloud/fog water (Lüttke et al., 1997; Harrison et al., 2005; Frka et al., 2016; Li et al., 2022; Liu et al., 2023a; Lian et al., 2021). The reactions might be influenced by the liquid water content (LWC) and the pH of the aqueous phase (Lian et al., 2021; Vidovic et al., 2018). For instance, a low pH would facilitate the formation of 2,4-dinitrophenols by nitration (Vione et al., 2005), but inhibits the reactions between glyoxal and reduced nitrogen (Sedehi et al., 2013; Yang et al., 2024). Aerosol liquid water and fog water are two crucial medias for the aqueous-phase reactions of organics, characterized by significant differences in LWC and pH (Ervens et al., 2011; Blando and Turpin, 2000). Due to the limited comprehensive studies of aqueous-phase processes in these two phases, the contribution of various secondary formation pathways to secondary NOCs remains unclear up to now.

Northern China has experienced severe haze pollution in recent years. Anthropogenic emissions, including BB, CC, and VE, have been identified as major contributors to the air pollution in this region (Li et al., 2019a; Li et al., 2023; Li et al., 2019b; Tang et al., 2020). High relative humidity has also been regarded as an important driver for secondary pollution in northern China (Xu et al., 2017; Kuang et al., 2020; Li et al., 2020a). However, research on their contribution to NOCs at the molecular level is scarce (Wang et al., 2019). In this study, pre-fog aerosols and fog water were collected during a severe

https://doi.org/10.5194/egusphere-2024-74
Preprint. Discussion started: 5 February 2024

haze period at a suburban site in northern China and analyzed using FT-ICR MS coupled with electrospray ionization (ESI) source in both negative and positive ionization modes. A good capture of NOCs molecules, up to 80%, can be expected by combining ESI+ and ESI- (Cape et al., 2011; Jiang et al., 2022). The primary NOCs from anthropogenic emission were identified, and the different formation pathways of NOCs in pre-fog aerosols and in fog water were discussed.

2 Materials and Methods

2.1 Sample collection and pretreatment

The sampling site is located in a suburban area in Qingdao, China (36.35°N, 120.68°E). It is surrounded by villages and is close to the coast. The aerosol and fog water samplers were installed on the roof of a four-story building. The environmental and meteorological conditions during the sampling campaign have been described elsewhere (Hu et al., 2022; Zhang et al., 2021).

A severe haze episode lasted from December 6 to December 11, 2019, during which the concentration of $PM_{2.5}$ reached up to 300 μg m^{-3} (Fig. S1). The fog event occurred on the morning of December 10 with visibility <100 m and relative humidity > 90%, lasting from ~06:30 to ~11:20 a.m. (Fig. S1). Two fog water samples (QDF1 and QDF2) were collected using a Caltech Active Strand Cloud water Collector, Version 2 (CASCC2). The flow rate of the CASCC2 was 5.8 m^3 min^{-1} and the collection efficiency was 86%. Collected fog water was filtered using polytetrafluoroethylene filters, and the pH of the fog water was measured on-site using a pH meter (Mettler Toledo, Switzerland). Then the samples were kept at -20 °C until analysis.

Two aerosol samples collected on December 8 and 9 before the fog event (labeled as pre-fog aerosols QDP1 and QDP2) were selected for comparative analysis with the fog water samples. Aerosols were collected daily onto quartz fiber filters with a radius of 45 mm (Pall, U.S.A.) using a $PM_{2.5}$ sampler (TH-150A, Wuhan Tianhong, China) at a flow rate of 100 L min^{-1}. The filters had been pretreated by baking in a muffle furnace at 450 °C for 4 hours to eliminate any organic contaminants before the sampling. The duration of sampling for each sample was set as ~23.5 hours, i.e., from 8:00 a.m. to ~7:30 a.m. the next day. Filters were refrigerated at -20 °C immediately after sampling.

For the FT-ICR MS analysis, one eighth of aerosol filters were cut into pieces, extracted with ultrapure water using ultrasonic agitation, and then filtered through 0.22 μm polytetrafluoroethylene filters. The water-soluble organic matter (WSOM) in fog water and water extracts from aerosols was isolated using a solid-phase extraction (SPE) process. The analytes were eluted from the SPE cartridges using a mixture of acetonitrile/methanol/ ultrapure water (45/45/10, *v*:*v*:*v*) at pH 10.4, and then redissolved in 1 mL of methanol before the instrumental analysis (as described in Text S1).

2.2 Instrumental analysis and data processing

The molecular composition of WSOM in fog water and aerosols was detected using an ESI source (Bruker Daltonik GmbH, Bremen, Germany) coupled with a 9.4-T solariX FT-ICR MS. Both negative and positive ionization modes of the ESI source

https://doi.org/10.5194/egusphere-2024-74
Preprint. Discussion started: 5 February 2024

were utilized. The mass range scanned was 100-800 Da. A total of 128 continuous 4M data FT-ICR transients were co-added to improve the signal-to-noise ratio and dynamic range. All mathematically possible formulas for ions with a signal-to-noise ratio greater than 10 were calculated, considering a mass tolerance of ± 0.6 ppm. The maximum numbers of atoms for the formula calculator were set to: 30 ^{12}C, 60 ^{1}H, 15 ^{16}O, 2 ^{14}N, 2 ^{32}S, 1 ^{13}C, 1 ^{18}O, and 1 ^{34}S for ESI- and one additional ^{23}Na for ESI+. Formulas assigned to isotopomers (i.e., ^{13}C, ^{18}O, or ^{34}S) were not discussed. The neutral molecular formula $C_cH_hO_oN_nS_s$ was achieved by adding H (in ESI-) or subtracting H or Na (in ESI+). Further screening was applied using the following criteria to exclude formulas not detected frequently in natural materials: O/C ≤ 1.2, 0.3 ≤ H/C ≤ 2.25, N/C ≤ 0.5, S/C ≤ 0.2, 2C + 2 > H, C + 2 > O, and obeying the N rule. Only sample ion peaks with intensities enhanced >100 times higher than those of the blank sample ion peaks were retained for further analysis. More detailed information about the instrumental analysis can be found in our previous studies (Sun et al., 2021; Sun et al., 2023) and in Text S2. The double-bond equivalent (DBE) of each assigned formula $C_cH_hO_oN_nS_s$ was calculated as follows:

$$DBE = (2c + 2 - h + n)/2$$

The oxidation state of carbon atoms (OS_C) was calculated based on the approximation described in Kroll et al. (2011) and Brege et al. (2018):

$$OS_C \approx 2\times o/c - h/c - 5\times n/c - 6\times s/c$$

For each sample, the average elemental ratios of oxygen, carbon, and hydrogen (i.e., O/C, H/C, etc.) and other characteristic parameters weighted by intensity were calculated as follow:

$$X = \Sigma(X_i \times Int_i)/\Sigma Int_i$$

where X_i and Int_i represent the parameter and intensity, respectively, in the mass spectrum of each individual molecular formula, *i*.

Water-soluble ions in fog water were analyzed using ion chromatography (883 Basic IC plus, Metrohm, Switzerland).

"Precursor-product pairs" were used to investigate the formation pathways of NOCs in this study. The chemical reactions of the precursor result in changes in the number of atoms within the molecule. Therefore, by adding or subtracting atoms in the precursor, the molecular formula of the product can be obtained. For example, if the precursor $C_cH_hO_oN_nS_s$ undergoes a nitration reaction (-H+NO_2), its corresponding product would be $C_cH_{h-1}O_{o+2}N_{n+1}S_s$. A total of 39 reaction pathways were considered in the analysis (Table S1) (Lian et al., 2020; Liu et al., 2023b). In pre-fog aerosols, the primary molecules were regarded as precursors, which were identified by comparing them with the datasets of the molecular composition of WSOM in BB (including corn, rice, and pine) and CC smoke detected by both ESI- and ESI+ coupled with FT-ICR MS, and VE detected by ESI- FT-ICR MS (Song et al., 2018; Tang et al., 2020; Song et al., 2021), and the other molecules were regarded as products. While in fog water, the activated molecules were regarded as precursors, which were identified by comparing them with the molecular list in pre-fog aerosols, and the unique molecules were regarded as products.

https://doi.org/10.5194/egusphere-2024-74
Preprint. Discussion started: 5 February 2024

3 Results and Discussion

3.1 Profiles of molecular composition in pre-fog aerosol and fog water

The reconstructed mass spectrogram of ESI- and ESI+ FT-ICR MS for a typical sample is shown in Fig. 1A. A total of 2659-3753 formulas in ESI- mode, and 1695-2419 formulas in ESI+ mode were assigned for two pre-fog aerosol samples. Four molecular groups (CHO-, CHON-, CHOS-, and CHONS-) were categorized based on the elemental compositions of molecular formulas in ESI-, while three groups (CHO+, CHN+, and CHON+) were categorized in ESI+ modes. The fractions of their numbers and relative abundance (f_{RA}, normalized by the sum of intensity) are presented in Figs. 1B and S2. CHON represents the most abundant group in both modes. The numbers of NOCs (CHON-, CHONS-, CHN+, and CHON+) are 1697-2397 in ESI- and 1387-2039 in ESI+, comprising number fractions of 63.8-63.9% (f_{RA} of 60.0-62.5%) and 81.8-84.3% (f_{RA} of 85.0-86.7%) in all assigned formulas, respectively. The significant contribution of NOCs to organic aerosols has also been observed at rural (Jiang et al., 2023; Mao et al., 2022) and urban sites (Jang et al., 2020) in northern China during haze events.

Similar profiles were also found in fog water. Totally, 3903-3992 formulas in ESI-, and 3011-3460 formulas in ESI+ mode, were assigned to fog water samples, including 2551-2633 and 2477-2845 NOCs, respectively. NOCs constitute high number fractions of 65.0-66.0% (f_{RA} of 69.7-75.0%) and 82.2-82.3% (f_{RA} of 84.1-85.7%) in all formulas in ESI- and ESI+, respectively (Figs. 1B and S2). The fractions are higher than those in cloud water at Mt. Tai, in which CHON accounts for 33% and 63% of all detected molecules in ESI- and ESI+ mode, respectively (Liu et al., 2023b). The high proportion of NOCs in this study may be related to the enhanced emissions and subsequent secondary formation, as discussed below.

The molecular characteristics of NOCs, including oxidation states, unsaturation, and molecular weight, in pre-fog aerosols and fog water are presented in Table 1. It is evident that molecules in ESI- exhibit higher oxidation state (O/C and OS_C), lower unsaturation (DBE), and lower molecular weight compared to those in ESI+. It is interesting to note that H/C of molecules in ESI- is lower than that in ESI+, seemingly an opposite trend of unsaturation with DBE. The plot of DBE versus H/C of CHON- and CHON+ clearly shows that CHON- usually has lower H/C than CHON+ (Fig. S3) at the same DBE value. We note the CHON+ has more abundant nitrogen atoms than CHON- (1.56 vs. 1.45 on average). The introduction of nitrogen into a molecule includes the possibility to form N–C π-bonds, and requires an additional H atom to fill the additional valence of nitrogen (Koch and Dittmar, 2006), which may lead to a high average H/C of CHON+.

Generally, the oxidation state of NOCs in fog water is similar to or slightly lower than that in aerosols, which is consistent with the findings of cloud water in southern China (Sun et al., 2021). This may be partially attributed to different secondary formation pathways, as discussed in Section 3.3. The DBE values and molecular weight of CHON-, CHON+, and CHN+ in fog water are lower than those in pre-fog aerosols, but is not the case for CHONS-. Some unique CHONS- molecules with high DBE (9-11) and molecular weight (>290) in fog water explain the higher average values (Fig. S4). The "precursor-product pair" analysis in Section 3.3 indicates that these molecules are likely formed primarily through dehydrogenation, dehydration, and other aqueous-phase reactions with the loss of hydrogen atoms in fog water.

https://doi.org/10.5194/egusphere-2024-74
Preprint. Discussion started: 5 February 2024

3.2 Primary sources attribution of NOCs in pre-fog aerosols

Molecules detected in two ionization modes exhibit significant differences. A total of 826 NOCs formulas were assigned in both ionization modes in two pre-fog aerosol samples, and 1050 in fog water samples, representing 22.2% and 22.1% of the total NOCs, respectively. The result indicates that the combination of ESI- and ESI+ will greatly expand the "Event Horizon" of the molecular compositions (Cooper et al., 2022). To ensure representativeness, molecules in two ionization modes will be combined to discuss the source and transformation of NOCs in the following text.

By comparing the molecular composition of primary anthropogenic emissions (Song et al., 2018; Tang et al., 2020; Song et al., 2021), the NOCs molecules in pre-fog aerosols were categorized into BB, CC, VE, and other sources. Similar methods have also been utilized for source attribution of the molecules detected in aerosols (Tang et al., 2022; Jiang et al., 2023; Mao et al., 2022). The number of NOCs derived from BB, CC, and VE is 2298, 1557, and 547, accounting for 61.7%, 41.8%, and 14.7% of the total NOCs, respectively. Some NOCs were assigned to more than one primary source. Totally, the primary anthropogenic sources (BB, CC, and VE) generated NOCs (pNOCs) accounts for 72.3% of the total NOCs in pre-fog aerosols. This suggests that anthropogenic emission significantly contributes to the species richness of particulate NOCs during the haze event at this suburban site.

The Van Krevelen (VK) diagram facilitates information retrieval from assigned molecules (Kim et al., 2003; Hockaday et al., 2009). In this study, the NOCs molecules from various sources were plotted on the VK diagram (Fig. 2). It is evident that primary anthropogenic NOCs are mainly distributed in the lower left corner, while NOCs from the other sources are in the upper right area (Fig. 2). Consistently, the average O/C and H/C of pNOCs are significantly lower than those of other sources (Fig. S5). Note that the dataset deficiency on the VE source in ESI+ may introduce uncertainty in assigning sources to molecules. However, our focus is on the overall trend of the secondary NOCs formation process, rather than individual molecules. More importantly, ESI+ tends to ionize molecules with fewer oxygen and more hydrogen. Therefore, even if the ESI+ molecules are included, the average O/C and H/C position of VE on the VK diagram would shift to the upper left direction. It won't change the relative position of "other sources" and pNOCs. NOCs from other sources have relatively higher O/C (0.65 ± 0.29), H/C (1.55 ± 0.42), as well as N/C (0.14 ± 0.07) compared with those from primary anthropogenic emissions (Fig. S5), which are similar to those of aged aerosols (Jiang et al., 2023). In addition, the contribution of other primary sources to particulate NOCs at this suburban site may be very limited during winter. Therefore, it is reasonable to consider these NOCs from other sources as the secondary NOCs.

3.3 The formation of secondary NOCs in pre-fog aerosols and fog water

To identify the pathways of secondary NOCs formed in pre-fog aerosol (saNOCs), the "precursor-product pairs" were screened from the formula list of pre-fog aerosols, in which the primary molecules (i.e., molecules corresponding to BB, CC, or VE emission) were regarded as precursors, and saNOCs were regarded as products. The products of 39 reaction pathways collectively account for 83% of saNOCs, demonstrating their representativeness. Most of the reaction pathways are related to

https://doi.org/10.5194/egusphere-2024-74
Preprint. Discussion started: 5 February 2024

the addition and subtraction of H, O, and C atoms to NOCs molecules, such as the oxygen addition and dealkylation. Two types of formation pathways of the asNOCs with nitrogen addition on nitrogen-free or one-nitrogen molecules are nitration ($-H+NO_2$, corresponding to nitro substitution) and NH_3 addition ($-O+NH$ and $-HO_2+N$). The NH_3 addition pathways include the amine pathway and intramolecular N-heterocycle pathway of reactions between carbonyl compounds and ammonia, indexed as NH3Add1 and NH3Add2 in the following texts, respectively (Table S1) (Liu et al., 2023b). As depicted in Fig. 3, three pathways (nitration, NH3Add1, and NH3Add2) produce 450, 228, and 120 asNOCs products, accounting for 43.6%, 22.1%, and 11.6% of all asNOCs, respectively. Since the ESI- and ESI+ modes preferentially ionize acidic and basic functional groups, respectively (Song et al., 2021), the number ratio of detected molecules between ESI+ and ESI- ($NR_{+/-}$) may reflect the functional groups of products to some extent. The $NR_{+/-}$ of nitration products in saNOCs is 0.16, significantly lower than that of NH_3 addition products (0.85 and 0.76 for NH3Add1 and NH3Add2, respectively, as shown on Table S2). The result is consistent with the fact that NH_3 addition would introduce the reduced nitrogen into the molecules, making it more easily detectable by ESI+.

The formation pathways of secondary NOCs formed in fog water (sfNOCs) was also evaluated, based on the assumption that fog droplets are formed through the hygroscopic activation of particulate matter. The common molecules between fog water and pre-fog aerosols (n = 4830) were assigned as the activated molecules, while the unique NOCs molecules in fog water (n = 1315) were labeled as sfNOCs, which is similar to previous study (Liu et al., 2023b). The sfNOCs molecules do not show significant differences in characteristic parameters (O/C and N/C) from activated NOCs molecules, expect for a slightly higher H/C in the former (Figs. S6 and S7). The activated molecules and sfNOCs were then regarded as precursors and products, respectively, in the "precursor-product pair" analysis. The products of 39 reaction pathways account for 91% of sfNOCs. As shown in Fig. 3, the distribution of reaction pathways in fog water is quite different from that in pre-fog aerosols. The contributions of these pathways are comparable to each other, except for the reaction of sulfur. For instance, the oxygen addition and the reaction of carboxylic acid result in the addition and loss of oxygen atoms, respectively (Fig. 3 and Table S1). The contribution to sfNOCs of these two pathways is of similar magnitude (23.3-28.2% and 22.7-29.6%, respectively), which may provide a reasonable explanation for the similar mean O/C between precursors and products in fog water. When examining the formation pathways of sfNOCs with nitrogen addition, it becomes apparent that two NH_3 addition pathways are comparable to the nitration pathway in fog water. Nitration, NH3Add1, and NH3Add2 produce 352, 374, and 390 sfNOC products, accounting for 26.8%, 28.4%, and 29.7% of all sfNOCs, respectively. It is therefore easy to conclude that nitration plays a more important role in the formation of NOCs in aerosols, but NH_3 addition in fog water. The $NR_{+/-}$ of the sfNOCs generated by these three pathways are 0.25, 0.84, and 0.78, respectively (Table S2), which is similar to that of asNOCs.

The varying contributions of formation pathways to secondary NOCs in pre-fog aerosols and fog water may be associated with the concentrations of nitrogen-containing species in the aqueous phase (e.g., NO_3^- and NH_4^+ concentrations), the distribution of organic precursors, and/or the properties of the aqueous phases (e.g., LWC and pH). First, the average NH_4^+/NO_3^- ratios in terms of mass concentration in two fog water samples were 0.45 and 0.57, respectively. The values are similar to those observed in the pre-fog aerosols, which is 0.45-0.68 for the fine particulates (<1 μm) and 0.51-0.66 for

https://doi.org/10.5194/egusphere-2024-74
Preprint. Discussion started: 5 February 2024

coarse particulates (>1 μm) (Zhang et al., 2021). Thus, the different pathways of NOCs formation cannot be explained by the variation of NH_4^+ and NO_3^- in two phases. Second, the NH_3 addition reactions can only occur on the carbonyl group, and therefore have higher selectivity than the nitration reaction. A closer glimpse at the organic compositions shows that the precursors in pre-fog aerosols consist of primary organics from BB, CC, and VE with a low average O/C of 0.39, while those in fog water are more oxidized organics (O/C = 0.46 on average), including both primary and secondary organics formed in pre-fog aerosols, which may allow more carbonyl groups (Fig. 2 and S6). Although it is virtually impossible to identify the functional groups in the formula list obtained by FT-ICR MS, carbonyls have been widely detected in fog and cloud water (Ervens et al., 2013; Van Pinxteren et al., 2005). More importantly, a high LWC in cloud water may promote the dissolution of some carbonyl compounds (e.g., methylglyoxal) from gas phase and increase their aqueous concentrations (Li et al., 2020b). The enhanced formation of imidazole, a typical product of carbonyls and ammonium/amine, was also observed in cloud droplets in southern China (Lian et al., 2021). It is therefore reasonable to speculate that the varying distributions of organic precursors in two phases may lead to different reaction pathways. Third, the varying acidity in pre-fog aerosols and fog water likely provides another plausible explanation for the different contributions of various formation pathways to secondary NOCs. The pH value of fog water in this study was detected as 5.1, while those of pre-fog aerosols were evaluated as less than 4.0 by the ISORROPIA-II model (Zhang et al., 2021). Such a difference in pH may lead to several times difference of reaction rates for the nitration and NH_3 addition pathways. For instance, the formation rate of 2,4-dinitrophenols from the nitration of 4-nitrophenol at pH 4 is 4.4 times higher than that at pH 5 (Vione et al., 2005), while the rate of reactions between glyoxal and ammonium sulfate at pH 5 is approximately 15 times higher than that at pH 4 (IUPAC, 2017).

3.4 The impact of secondary processes on compositions of NOCs

To assess the influence of secondary processes on the molecular composition of NOCs, we categorized NOCs into seven classes in the VK plot (Table S3) (Bianco et al., 2018). A heatmap plotted based on the molecular classes clearly illustrates the variations in the distribution of pNOCs, saNOCs, and sfNOCs (Fig. 4A). The pNOCs in pre-fog aerosols are predominantly composed of CRAMs-like structures (61.4%), while saNOCs are enhanced in carbohydrates-like (28.3% in saNOCs vs 3.8% in pNOCs) and highly oxygenated compounds (HOCs, 25.2% in saNOCs vs 4.6% in pNOCs), corresponding to the higher oxidation state and saturation of saNOCs. Meanwhile, sfNOCs have a significantly higher number fraction of lipids-like compounds (21.4%) compared to pNOCs (8.0%).

The different composition of saNOCs and sfNOCs is a result of distinct formation pathways in two phases. The distribution of nitration products in pre-fog aerosols, of which 37.5% is HOCs, is consistent with that of all saNOCs (Fig.4A), suggesting that the nitration reaction in aerosols significantly contribute to the presence of highly oxygenated NOCs. Moreover, in this study, the average relative humidity during the pre-fog aerosol collection is 70 ± 14% (Fig. S1). Such a high RH may be beneficial for the formation of HOCs in aerosol liquid water, as evidenced by the observation of aqueous-phase formation of oxygenated organic aerosol during the haze in the North China Plain (Feng et al., 2022; Kuang et al., 2020; Xu et al., 2017).

https://doi.org/10.5194/egusphere-2024-74
Preprint. Discussion started: 5 February 2024

Conversely, the NH_3 addition reactions in pre-fog aerosols mainly enhance aliphatic/peptides-like compounds (Fig. 4A). Applying the same method to fog water, the NH3Add1 and NH3Add2 products enhance lipids-like NOCs (19.0% and 21.2%), while nitration products were dominated by HOCs (42.9%). The former plays a more important role in shaping the composition of sfNOCs since they have a more similar distribution (Fig. 4A).

Dividing NOCs into different subclasses based on the distribution of characteristic elements (N, O, and S) can further provide insights into molecular composition. The distribution of CHON molecule subclasses is shown in Fig. 4B. The pNOCs follow an approximate normal distribution with peaks at $-N_1O_7$ and $-N_2O_6$ for one- and two-nitrogen molecules ($-N_1$ and $-N_2$), respectively. In saNOCs, the fraction of $-N_1$ NOCs decreases while that of $-N_2$ NOCs (e.g., $-N_2O_{5\text{-}7,10\text{-}12}$) increases. While a lower content of oxygen atoms was observed in sfNOCs, with peaks at $-N_1O_5$ and $-N_2O_3$ (Fig. 4B).

Nitration and NH_3 addition in pre-fog aerosols might contribute to the enhancement of $-N_2O_{10\text{-}12}$ and $-N_2O_{5\text{-}7}$, respectively. The high ratio of O/N in these NOCs indicates the existence of $-NO_2$ or $-ONO_2$ (Leclair et al., 2012; Song et al., 2021). However, the NH_3 addition products may contain both reduced nitrogen and other oxidized functional groups. The excess oxygen atoms may mainly exist in the form of oxygen-containing functional groups, such as -OH and -COOH (Tang et al., 2022; Yang et al., 2023). In fog water, nitration and NH_3 addition also mainly contribute to high- and low-oxygen-number molecules, respectively, and NH_3 addition products have a similar distribution to all the sfNOCs.

In addition, the heatmap illustrating the distribution of CHONS is shown in Fig. S8, in which the same conclusion can be easily drawn, namely, NH_3 addition reactions play a more significant role in shaping the composition of sfNOCs. The numbers of CHN in sfNOCs (n = 29) is higher than in saNOCs (n = 8), which is also the result of the increased contribution from NH_3 addition in fog water.

4 Conclusions

A case study was conducted on the composition of NOCs in pre-fog aerosols and fog water at a suburban site in the North China Plain during a winter haze episode. NOCs make up more than 60% of all molecular formulas assigned by both ESI- and ESI+ modes coupled with FT-ICR MS, indicating a significant contribution of NOCs to the haze pollution. The primary anthropogenic emissions are the dominant contributor to the species richness of NOCs in pre-fog aerosols, accounting for >70% of the number fraction. The secondary aqueous pathways explain the remaining fraction. The nitration reaction plays a dominant role in secondary NOCs formation in aerosols, while the NH_3 addition pathways are more important in fog water. As a result, the secondary NOCs in aerosols contain a high abundance of HOCs and carbohydrates compounds with nitrogen in the form of $-NO_2$ or $-ONO_2$ compared to primary NOCs. Differently, secondary NOCs formed in fog water are associated with increased lipids-like compounds, which may contain more abundant reduced nitrogen. It is important to note that our findings may represent the phenomena under specific conditions due to the limited sample size. Nevertheless, the results reveal the diverse impact of chemical processes in aerosols and fog water on the composition of NOCs at a molecular level, which is valuable for assessing the environmental and climatic effects of NOCs.

https://doi.org/10.5194/egusphere-2024-74
Preprint. Discussion started: 5 February 2024

Supplement. Supporting information includes two texts (Text S1-2), eight figures (Fig. S1-S8), and three tables (Table S1-3) related to the manuscript.

Data availability. The raw data of this study can be obtained by contacting the corresponding author.

Author contributions. XB and GZ design the research with input from XW and PP. WS, XH, and YF collected samples. WS and BJ carried out the sample pretreatment and instrumental analysis under the guidance of YL. WS processed data, and wrote the manuscript. XB, and GZ interpreted data and edited the manuscript. LX, CY, XW, YZ, and HM had an active role in supporting the sampling work. All authors contributed to the discussions of the results and refinement of the manuscript.

Competing interests. The authors declare that they have no conflict of interest.

Financial support. This work was funded by the National Key Research and Development Program of China (2022YFC3701103 and 2023YFC3710100), National Funded Postdoctoral Researcher Program (GZC20232683), National Natural Science Foundation of China (42222705 and 42130611), Youth Innovation Promotion Association CAS (2021354), and Guangdong Foundation for Program of Science and Technology Research (2023B1212060049).

https://doi.org/10.5194/egusphere-2024-74
Preprint. Discussion started: 5 February 2024

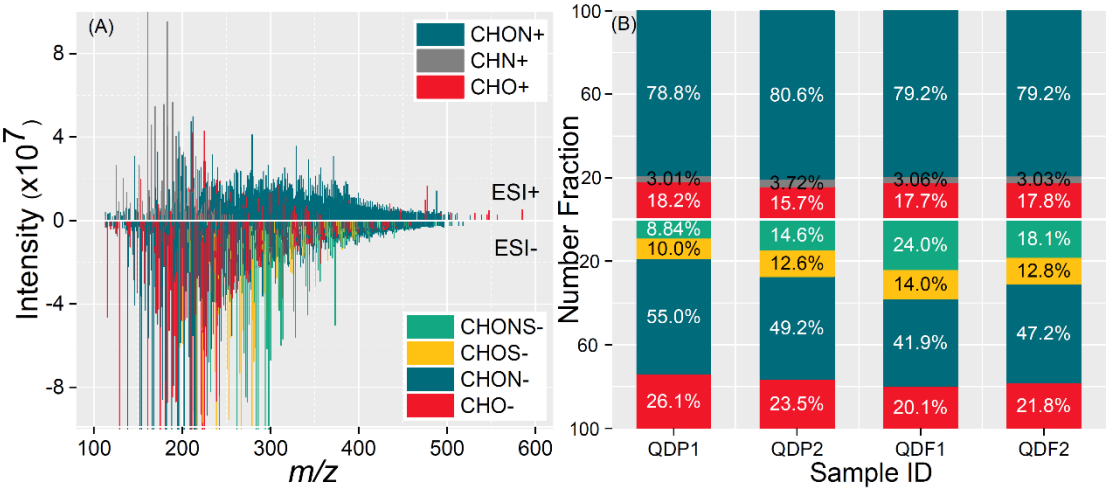

Figure 1: Panel A: The reconstructed mass spectrogram of a typical aerosol sample QDP1. The negative and positive values of the y-axis represent the intensities of the ion peaks detected in ESI- and ESI+, respectively. Panel B: The number fraction of each molecular group in ESI- and ESI+ mode.

https://doi.org/10.5194/egusphere-2024-74
Preprint. Discussion started: 5 February 2024

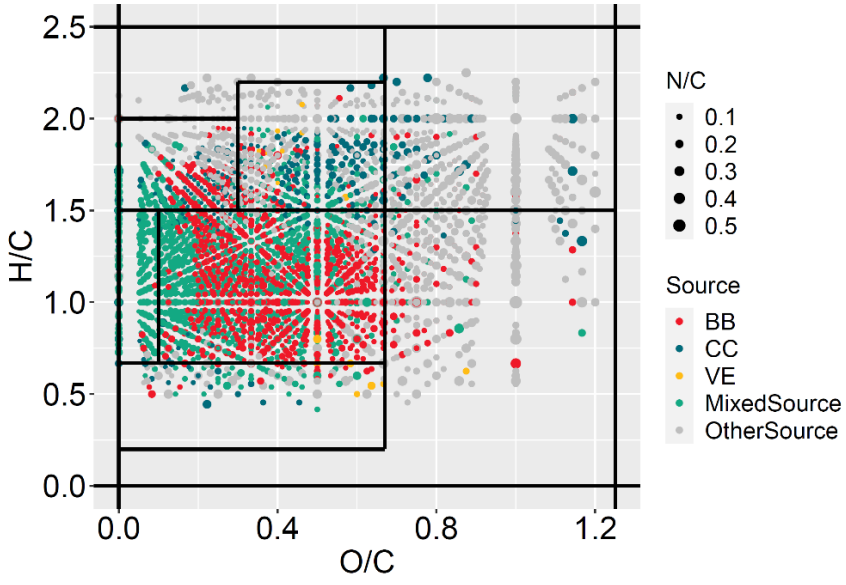

315

Figure 2: The Van Krevelen diagrams for NOCs from different sources (Biomass burning, BB; Coal combustion, CC; Vehicle emission, VE, and other sources, OtherSource) in pre-fog aerosols. The "MixedSource" in the plot represents the molecules were assigned to at least two sources of BB, CC, and VE.

https://doi.org/10.5194/egusphere-2024-74
Preprint. Discussion started: 5 February 2024

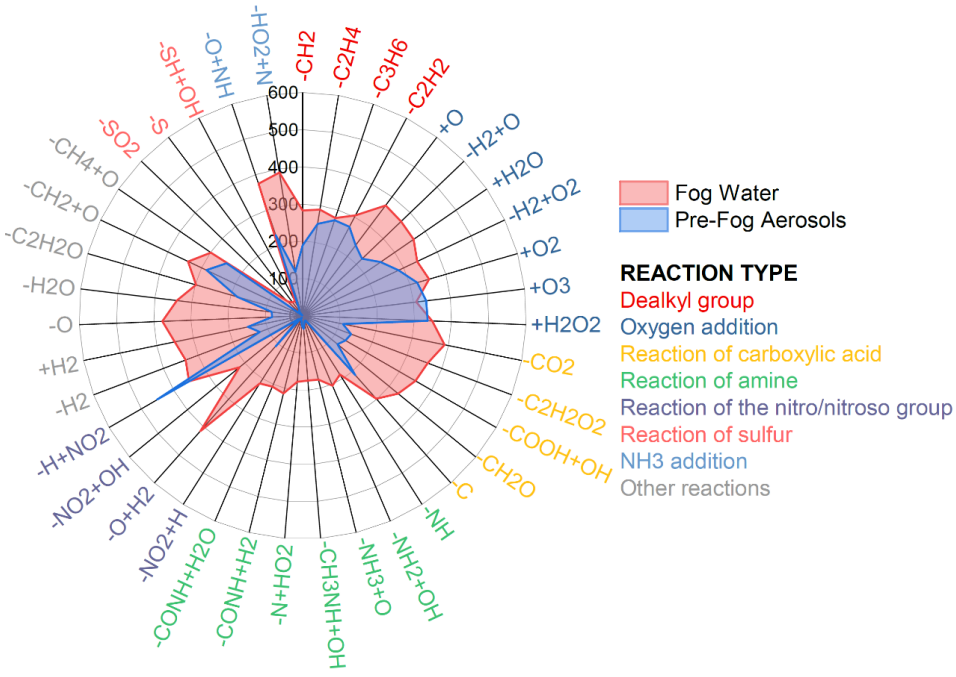

Figure 3: Radar plot of the links from precursors (pNOCs) to products (saNOCs and sfNOCs) in pre-fog aerosols and fog water based on 39 reaction pathways. The y-axis (0-600) in the plot represent the number of "precursor-product pair".

https://doi.org/10.5194/egusphere-2024-74
Preprint. Discussion started: 5 February 2024

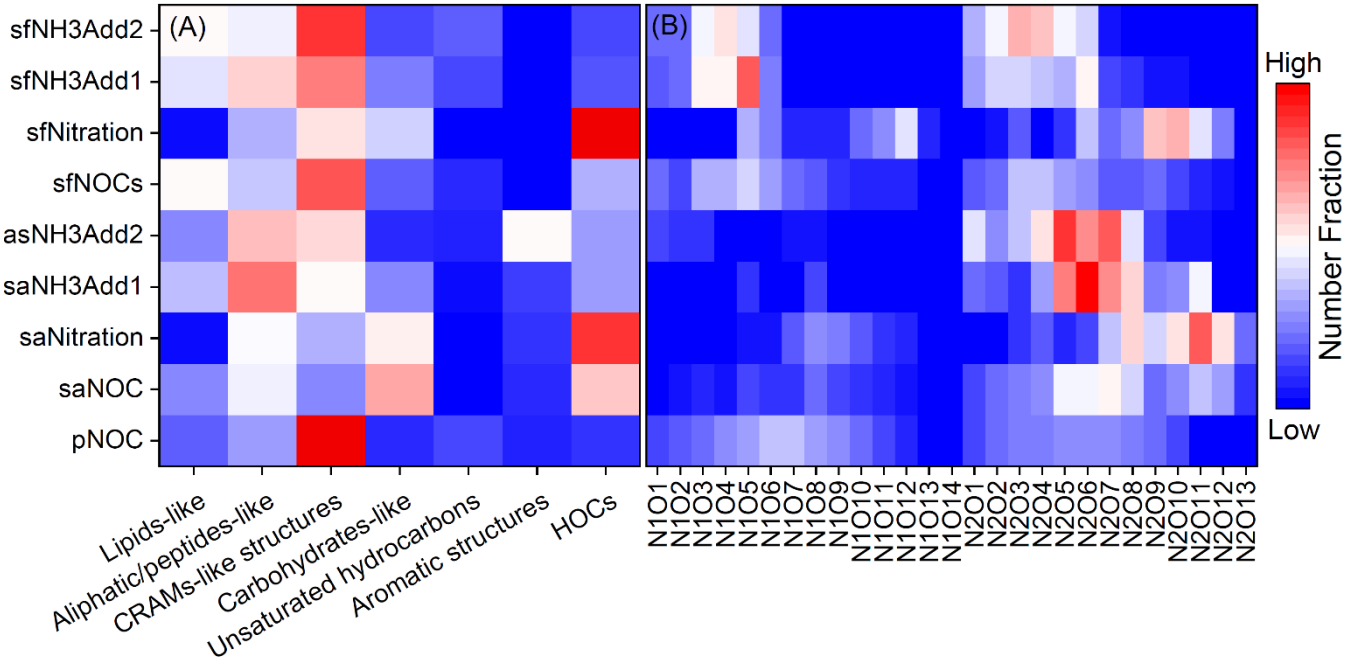

Figure 4: The heatmap of seven classes of NOCs divided by O/C and H/C (panel A) and subclasses of CHON divided by the number of N and O atoms in pNOCs, all saNOCs, all sfNOCs, and nitration- and NH_3 addition- formed NOCs (panel B).

https://doi.org/10.5194/egusphere-2024-74
Preprint. Discussion started: 5 February 2024

Table 1: The ranges of the relative-abundance-weighted average values of the parameters (including O/C, OS_C, H/C, DBE, #C and MW)

		O/C	OS_C	H/C	DBE	#C	MW
Pre-Fog Aerosol	CHON-	0.51-0.57	-0.66~-0.67	1.05-1.17	6.42-6.54	10.75-11.81	242.2-277.7
	CHON+	0.31-0.34	-1.17~-1.03	1.32-1.41	6.68-7.52	17.24-17.30	332.6-340.9
	CHONS-	0.81-0.86	-1.29~-1.23	1.65-1.76	2.67-3.30	9.51-10.09	304.0-311.5
	CHN+	--	--	1.30-1.31	6.16-6.18	11.92-11.96	184.7-185.1
Fog Water	CHON-	0.59-0.59	-0.77~-0.73	0.98-1.02	5.82-5.96	8.47-9.19	207.8-222.9
	CHON+	0.31-0.31	-1.39~-1.38	1.46-1.47	6.07-6.20	15.89-15.96	309.8-310.0
	CHONS-	0.78-0.81	-1.22~-1.21	1.53-1.63	3.49-4.10	10.27-10.41	313.7-316.7
	CHN+	--	--	1.39-1.47	5.07-5.52	11.36-11.85	176.4-181.2

https://doi.org/10.5194/egusphere-2024-74
Preprint. Discussion started: 5 February 2024

References

Altieri, K. E., Hastings, M. G., Peters, A. J., and Sigman, D. M.: Molecular characterization of water soluble organic nitrogen in marine rainwater by ultra-high resolution electrospray ionization mass spectrometry, Atmos. Chem. Phys., 12, 3557-3571, http://doi.org/10.5194/acp-12-3557-2012, 2012.

Bianco, A., Deguillaume, L., Vaitilingom, M., Nicol, E., Baray, J. L., Chaumerliac, N., and Bridoux, M.: Molecular Characterization of Cloud Water Samples Collected at the Puy de Dome (France) by Fourier Transform Ion Cyclotron Resonance Mass Spectrometry, Environ. Sci. Technol., 52, 10275-10285, http://doi.org/10.1021/acs.est.8b01964, 2018.

Blando, J. D. and Turpin, B. J.: Secondary organic aerosol formation in cloud and fog droplets: a literature evaluation of plausibility, Atmos. Environ., 34, 1623-1632, http://doi.org/10.1016/S1352-2310(99)00392-1, 2000.

Boone, E. J., Laskin, A., Laskin, J., Wirth, C., Shepson, P. B., Stirm, B. H., and Pratt, K. A.: Aqueous Processing of Atmospheric Organic Particles in Cloud Water Collected via Aircraft Sampling, Environ. Sci. Technol., 49, 8523-8530, http://doi.org/10.1021/acs.est.5b01639, 2015.

Brege, M., Paglione, M., Gilardoni, S., Decesari, S., Facchini, M. C., and Mazzoleni, L. R.: Molecular insights on aging and aqueous-phase processing from ambient biomass burning emissions-influenced Po Valley fog and aerosol, Atmos. Chem. Phys., 18, 13197-13214, http://doi.org/10.5194/acp-18-13197-2018, 2018.

Cai, Y., Ye, C., Chen, W., Hu, W., Song, W., Peng, Y., Huang, S., Qi, J., Wang, S., Wang, C., Wu, C., Wang, Z., Wang, B., Huang, X., He, L., Gligorovski, S., Yuan, B., Shao, M., and Wang, X.: The important contribution of secondary formation and biomass burning to oxidized organic nitrogen (OON) in a polluted urban area: insights from in situ measurements of a chemical ionization mass spectrometer (CIMS), Atmos. Chem. Phys., 23, 8855-8877, http://doi.org/10.5194/acp-23-8855-2023, 2023.

Cape, J. N., Cornell, S. E., Jickells, T. D., and Nemitz, E.: Organic nitrogen in the atmosphere — Where does it come from? A review of sources and methods, Atmos. Res., 102, 30-48, http://doi.org/10.1016/j.atmosres.2011.07.009, 2011.

Cooper, W. T., Chanton, J. C., D'Andrilli, J., Hodgkins, S. B., Podgorski, D. C., Stenson, A. C., Tfaily, M. M., and Wilson, R. M.: A History of Molecular Level Analysis of Natural Organic Matter by FTICR Mass Spectrometry and The Paradigm Shift in Organic Geochemistry, Mass. Spectrom. Rev., 41, 215-239, http://doi.org/10.1002/mas.21663, 2022.

De Haan, D. O., Corrigan, A. L., Smith, K. W., Stroik, D. R., Turley, J. J., Lee, F. E., Tolbert, M. A., Jimenez, J. L., Cordova, K. E., and Ferrell, G. R.: Secondary Organic Aerosol-Forming Reactions of Glyoxal with Amino Acids, Environ. Sci. Technol., 43, 2818-2824, http://doi.org/10.1021/es803534f, 2009.

De Haan, D. O., Tapavicza, E., Riva, M., Cui, T., Surratt, J. D., Smith, A. C., Jordan, M. C., Nilakantan, S., Almodovar, M., Stewart, T. N., de Loera, A., De Haan, A. C., Cazaunau, M., Gratien, A., Pangui, E., and Doussin, J. F.: Nitrogen-Containing, Light-Absorbing Oligomers Produced in Aerosol Particles Exposed to Methylglyoxal, Photolysis, and Cloud Cycling, Environ. Sci. Technol., 52, 4061-4071, http://doi.org/10.1021/acs.est.7b06105, 2018.

https://doi.org/10.5194/egusphere-2024-74
Preprint. Discussion started: 5 February 2024

Ditto, J. C., Machesky, J., and Gentner, D. R.: Analysis of reduced and oxidized nitrogen-containing organic compounds at a coastal site in summer and winter, Atmos. Chem. Phys., 22, 3045-3065, http://doi.org/10.5194/acp-22-3045-2022, 2022.

Ervens, B., Turpin, B. J., and Weber, R. J.: Secondary organic aerosol formation in cloud droplets and aqueous particles (aqSOA): a review of laboratory, field and model studies, Atmos. Chem. Phys., 11, 11069-11102, http://doi.org/10.5194/acp-11-11069-2011, 2011.

Ervens, B., Wang, Y., Eagar, J., Leaitch, W. R., Macdonald, A. M., Valsaraj, K. T., and Herckes, P.: Dissolved organic carbon (DOC) and select aldehydes in cloud and fog water: the role of the aqueous phase in impacting trace gas budgets, Atmos. Chem. Phys., 13, 5117-5135, http://doi.org/10.5194/acp-13-5117-2013, 2013.

Feng, S., Zhang, L., Wang, S., Nadykto, A. B., Xu, Y., Shi, Q., Jiang, B., and Qian, W.: Characterization of dissolved organic nitrogen in wet deposition from Lake Erhai basin by using ultrahigh resolution FT-ICR mass spectrometry, Chemosphere, 156, 438-445, http://doi.org/10.1016/j.chemosphere.2016.04.039, 2016.

Feng, Z., Liu, Y., Zheng, F., Yan, C., Fu, P., Zhang, Y., Lian, C., Wang, W., Cai, J., Du, W., Chu, B., Wang, Y., Kangasluoma, J., Bianchi, F., Petäjä, T., and Kulmala, M.: Highly oxidized organic aerosols in Beijing: Possible contribution of aqueous-phase chemistry, Atmos. Environ., 273, http://doi.org/10.1016/j.atmosenv.2022.118971, 2022.

Frka, S., Sala, M., Kroflic, A., Hus, M., Cusak, A., and Grgic, I.: Quantum Chemical Calculations Resolved Identification of Methylnitrocatechols in Atmospheric Aerosols, Environ Sci Technol, 50, 5526-5535, http://doi.org/10.1021/acs.est.6b00823, 2016.

Harrison, M. A. J., Barra, S., Borghesi, D., Vione, D., Arsene, C., and Iulian Olariu, R.: Nitrated phenols in the atmosphere: a review, Atmos. Environ., 39, 231-248, http://doi.org/10.1016/j.atmosenv.2004.09.044, 2005.

Hockaday, W. C., Purcell, J. M., Marshall, A. G., Baldock, J. A., and Hatcher, P. G.: Electrospray and photoionization mass spectrometry for the characterization of organic matter in natural waters: a qualitative assessment, Limno. Oceanogr. - Meth., 7, 81-95, http://doi.org/10.4319/lom.2009.7.81, 2009.

Hu, X., Guo, Z., Sun, W., Lian, X., Fu, Y., Meng, H., Zhu, Y., Zhang, G., Wang, X., Xue, L., Bi, X., Wang, X., and Peng, P. a.: Atmospheric Processing of Particulate Imidazole Compounds Driven by Photochemistry, Environ. Sci. Technol. Lett., 9, 265-271, http://doi.org/10.1021/acs.estlett.2c00029, 2022.

Huang, R. J., Yang, L., Shen, J., Yuan, W., Gong, Y., Guo, J., Cao, W., Duan, J., Ni, H., Zhu, C., Dai, W., Li, Y., Chen, Y., Chen, Q., Wu, Y., Zhang, R., Dusek, U., O'Dowd, C., and Hoffmann, T.: Water-Insoluble Organics Dominate Brown Carbon in Wintertime Urban Aerosol of China: Chemical Characteristics and Optical Properties, Environ. Sci. Technol., 54, 7836-7847, http://doi.org/10.1021/acs.est.0c01149, 2020.

IUPAC: IUPAC Task Group on Atmospheric Chemical Kinetic Data Evaluation [dataset], http://iupac.pole-ether.fr, 2017.

Jang, K. S., Choi, M., Park, M., Park, M. H., Kim, Y. H., Seo, J., Wang, Y., Hu, M., Bae, M. S., and Park, K.: Assessment of PM(2.5)-bound nitrogen-containing organic compounds (NOCs) during winter at urban sites in China and Korea, Environ. Pollut., 265, 114870, http://doi.org/10.1016/j.envpol.2020.114870, 2020.

https://doi.org/10.5194/egusphere-2024-74
Preprint. Discussion started: 5 February 2024

Jiang, H., Li, J., Sun, R., Tian, C., Tang, J., Jiang, B., Liao, Y., Chen, C. E., and Zhang, G.: Molecular Dynamics and Light Absorption Properties of Atmospheric Dissolved Organic Matter, Environ. Sci. Technol., 55, 10268-10279, http://doi.org/10.1021/acs.est.1c01770, 2021.

Jiang, H., Li, J., Tang, J., Zhao, S., Chen, Y., Tian, C., Zhang, X., Jiang, B., Liao, Y., and Zhang, G.: Factors Influencing the Molecular Compositions and Distributions of Atmospheric Nitrogen-Containing Compounds, J. Geophys. Res.: Atmos., 127, http://doi.org/10.1029/2021jd036284, 2022.

Jiang, H., Cai, J., Feng, X., Chen, Y., Wang, L., Jiang, B., Liao, Y., Li, J., Zhang, G., Mu, Y., and Chen, J.: Aqueous-Phase Reactions of Anthropogenic Emissions Lead to the High Chemodiversity of Atmospheric Nitrogen-Containing Compounds during the Haze Event, Environ. Sci. Technol., http://doi.org/10.1021/acs.est.3c06648, 2023.

Jimenez, N. G., Sharp, K. D., Gramyk, T., Ugland, D. Z., Tran, M.-K., Rojas, A., Rafla, M. A., Stewart, D., Galloway, M. M., Lin, P., Laskin, A., Cazaunau, M., Pangui, E., Doussin, J.-F., and De Haan, D. O.: Radical-Initiated Brown Carbon Formation in Sunlit Carbonyl–Amine–Ammonium Sulfate Mixtures and Aqueous Aerosol Particles, ACS Earth Space Chem., 6, 228-238, http://doi.org/10.1021/acsearthspacechem.1c00395, 2022.

Kim, H., Collier, S., Ge, X., Xu, J., Sun, Y., Jiang, W., Wang, Y., Herckes, P., and Zhang, Q.: Chemical processing of water-soluble species and formation of secondary organic aerosol in fogs, Atmos. Environ., 200, 158-166, http://doi.org/10.1016/j.atmosenv.2018.11.062, 2019.

Kim, S., Kramer, R. W., and Hatcher, P. G.: Graphical Method for Analysis of Ultrahigh-Resolution Broadband Mass Spectra of Natural Organic Matter, the Van Krevelen Diagram, Anal. Chem., 75, 5336-5344, http://doi.org/10.1021/ac034415p, 2003.

Koch, B. P. and Dittmar, T.: From mass to structure: an aromaticity index for high-resolution mass data of natural organic matter, Rapid Commun. Mass Sp., 20, 926-932, http://doi.org/10.1002/rcm.2386, 2006.

Kroflic, A., Grilc, M., and Grgic, I.: Does toxicity of aromatic pollutants increase under remote atmospheric conditions?, Sci. Rep., 5, 8859, http://doi.org/10.1038/srep08859, 2015.

Kroll, J. H., Donahue, N. M., Jimenez, J. L., Kessler, S. H., Canagaratna, M. R., Wilson, K. R., Altieri, K. E., Mazzoleni, L. R., Wozniak, A. S., Bluhm, H., Mysak, E. R., Smith, J. D., Kolb, C. E., and Worsnop, D. R.: Carbon oxidation state as a metric for describing the chemistry of atmospheric organic aerosol, Nat. Chem., 3, 133-139, http://doi.org/10.1038/nchem.948, 2011.

Kua, J., Krizner, H. E., and De Haan, D. O.: Thermodynamics and kinetics of imidazole formation from glyoxal, methylamine, and formaldehyde: a computational study, J. Phys. Chem. A, 115, 1667-1675, http://doi.org/10.1021/jp111527x, 2011.

Kuang, Y., He, Y., Xu, W., Yuan, B., Zhang, G., Ma, Z., Wu, C., Wang, C., Wang, S., Zhang, S., Tao, J., Ma, N., Su, H., Cheng, Y., Shao, M., and Sun, Y.: Photochemical Aqueous-Phase Reactions Induce Rapid Daytime Formation of Oxygenated Organic Aerosol on the North China Plain, Environ. Sci. Technol., 54, 3849-3860, http://doi.org/10.1021/acs.est.9b06836, 2020.

https://doi.org/10.5194/egusphere-2024-74
Preprint. Discussion started: 5 February 2024

Leclair, J. P., Collett, J. L., and Mazzoleni, L. R.: Fragmentation analysis of water-soluble atmospheric organic matter using ultrahigh-resolution FT-ICR mass spectrometry, Environ. Sci. Technol., 46, 4312-4322, http://doi.org/10.1021/es203509b, 2012.

Li, D., Wu, C., Zhang, S., Lei, Y., Lv, S., Du, W., Liu, S., Zhang, F., Liu, X., Liu, L., Meng, J., Wang, Y., Gao, J., and Wang, G.: Significant coal combustion contribution to water-soluble brown carbon during winter in Xingtai, China: Optical properties and sources, J. Environ. Sci. (China), 124, 892-900, http://doi.org/10.1016/j.jes.2022.02.026, 2023.

Li, J., Liu, Z., Gao, W., Tang, G., Hu, B., Ma, Z., and Wang, Y.: Insight into the formation and evolution of secondary organic aerosol in the megacity of Beijing, China, Atmos. Environ., 220, 117070, http://doi.org/10.1016/j.atmosenv.2019.117070, 2020a.

Li, J., Wang, G., Zhang, Q., Li, J., Wu, C., Jiang, W., Zhu, T., and Zeng, L.: Molecular characteristics and diurnal variations of organic aerosols at a rural site in the North China Plain with implications for the influence of regional biomass burning, Atmos. Chem. Phys., 19, 10481-10496, http://doi.org/10.5194/acp-19-10481-2019, 2019a.

Li, M., Fan, X., Zhu, M., Zou, C., Song, J., Wei, S., Jia, W., and Peng, P.: Abundance and Light Absorption Properties of Brown Carbon Emitted from Residential Coal Combustion in China, Environ. Sci. Technol., 53, 595-603, http://doi.org/10.1021/acs.est.8b05630, 2019b.

Li, M., Wang, X., Zhao, Y., Du, P., Li, H., Li, J., Shen, H., Liu, Z., Jiang, Y., Chen, J., Bi, Y., Zhao, Y., Xue, L., Wang, Y., Chen, J., and Wang, W.: Atmospheric Nitrated Phenolic Compounds in Particle, Gaseous, and Aqueous Phases During Cloud Events at a Mountain Site in North China: Distribution Characteristics and Aqueous-Phase Formation, J. Geophys. Res.: Atmos., 127, http://doi.org/10.1029/2022jd037130, 2022.

Li, T., Wang, Z., Wang, Y., Wu, C., Liang, Y., Xia, M., Yu, C., Yun, H., Wang, W., Wang, Y., Guo, J., Herrmann, H., and Wang, T.: Chemical characteristics of cloud water and the impacts on aerosol properties at a subtropical mountain site in Hong Kong SAR, Atmos. Chem. Phys., 20, 391–407, http://doi.org/10.5194/acp-2019-481, 2020b.

Li, X., Wang, Y., Hu, M., Tan, T., Li, M., Wu, Z., Chen, S., and Tang, X.: Characterizing chemical composition and light absorption of nitroaromatic compounds in the winter of Beijing, Atmos. Environ., 237, 117712, http://doi.org/10.1016/j.atmosenv.2020.117712, 2020c.

Lian, L., Yan, S., Zhou, H., and Song, W.: Overview of the Phototransformation of Wastewater Effluents by High-Resolution Mass Spectrometry, Environ. Sci. Technol., 54, 1816-1826, http://doi.org/10.1021/acs.est.9b04669, 2020.

Lian, X., Zhang, G., Yang, Y., Lin, Q., Fu, Y., Jiang, F., Peng, L., Hu, X., Chen, D., Wang, X., Peng, P. a., Sheng, G., and Bi, X.: Evidence for the Formation of Imidazole from Carbonyls and Reduced Nitrogen Species at the Individual Particle Level in the Ambient Atmosphere, Environ. Sci. Technol. Lett., 8, 9-15, http://doi.org/10.1021/acs.estlett.0c00722, 2021.

Liu, X., Wang, H., Wang, F., Lv, S., Wu, C., Zhao, Y., Zhang, S., Liu, S., Xu, X., Lei, Y., and Wang, G.: Secondary Formation of Atmospheric Brown Carbon in China Haze: Implication for an Enhancing Role of Ammonia, Environ. Sci. Technol., http://doi.org/10.1021/acs.est.3c03948, 2023a.

https://doi.org/10.5194/egusphere-2024-74
Preprint. Discussion started: 5 February 2024

Liu, Z., Zhu, B., Zhu, C., Ruan, T., Li, J., Chen, H., Li, Q., Wang, X., Wang, L., Mu, Y., Collett, J., George, C., Wang, Y., Wang, X., Su, J., Yu, S., Mellouki, A., Chen, J., and Jiang, G.: Abundant nitrogenous secondary organic aerosol formation accelerated by cloud processing, iScience, 26, http://doi.org/10.1016/j.isci.2023.108317, 2023b.

Lüttke, J., Scheer, V., Levsen, K., Wu¨ nsch, G., Cape, J. N., Hargreaves, K. J., Storeton-West, R. L., Acker, K., Wieprecht, W., and Jones, B.: Occurrence and formation of nitrated phenols in and out of cloud, Atmos. Environ., 2637–2648, http://doi.org/10.1016/S1352-2310(96)00229-4, 1997.

Mao, J., Cheng, Y., Bai, Z., Zhang, W., Zhang, L., Chen, H., Wang, L., Li, L., and Chen, J.: Molecular characterization of nitrogen-containing organic compounds in the winter North China Plain, Sci. Total Environ., 838, 156189, http://doi.org/10.1016/j.scitotenv.2022.156189, 2022.

Sedehi, N., Takano, H., Blasic, V. A., Sullivan, K. A., and De Haan, D. O.: Temperature- and pH-dependent aqueous-phase kinetics of the reactions of glyoxal and methylglyoxal with atmospheric amines and ammonium sulfate, Atmos. Environ., 77, 656-663, http://doi.org/https://doi.org/10.1016/j.atmosenv.2013.05.070, 2013.

Song, J., Li, M., Jiang, B., Wei, S., Fan, X., and Peng, P.: Molecular Characterization of Water-Soluble Humic like Substances in Smoke Particles Emitted from Combustion of Biomass Materials and Coal Using Ultrahigh-Resolution Electrospray Ionization Fourier Transform Ion Cyclotron Resonance Mass Spectrometry, Environ. Sci. Technol., 52, 2575-2585, http://doi.org/10.1021/acs.est.7b06126, 2018.

Song, J., Li, M., Zou, C., Cao, T., Fan, X., Jiang, B., Yu, Z., Jia, W., and Peng, P.: Molecular Characterization of Nitrogen-Containing Compounds in Humic-like Substances Emitted from Biomass Burning and Coal Combustion, Environ. Sci. Technol., http://doi.org/10.1021/acs.est.1c04451, 2021.

Song, J., Li, M., Fan, X., Zou, C., Zhu, M., Jiang, B., Yu, Z., Jia, W., Liao, Y., and Peng, P.: Molecular Characterization of Water- and Methanol-Soluble Organic Compounds Emitted from Residential Coal Combustion Using Ultrahigh-Resolution Electrospray Ionization Fourier Transform Ion Cyclotron Resonance Mass Spectrometry, Environ. Sci. Technol., 53, 13607-13617, http://doi.org/10.1021/acs.est.9b04331, 2019.

Sun, W., Guo, Z., Peng, X., Lin, J., Fu, Y., Yang, Y., Zhang, G., Jiang, B., Liao, Y., Chen, D., Wang, X., and Bi, X.: Molecular characteristics, sources and transformation of water-insoluble organic matter in cloud water, Environ. Pollut., 325, http://doi.org/10.1016/j.envpol.2023.121430, 2023.

Sun, W., Fu, Y., Zhang, G., Yang, Y., Jiang, F., Lian, X., Jiang, B., Liao, Y., Bi, X., Chen, D., Chen, J., Wang, X., Ou, J., Peng, P. a., and Sheng, G.: Measurement report: Molecular characteristics of cloud water in southern China and insights into aqueous-phase processes from Fourier transform ion cyclotron resonance mass spectrometry, Atmos. Chem. Phys., 21, 16631-16644, http://doi.org/10.5194/acp-21-16631-2021, 2021.

Tang, J., Li, J., Su, T., Han, Y., Mo, Y., Jiang, H., Cui, M., Jiang, B., Chen, Y., Tang, J., Song, J., Peng, P., amp, apos, an, and Zhang, G.: Molecular compositions and optical properties of dissolved brown carbon in biomass burning, coal combustion, and vehicle emission aerosols illuminated by excitation-emission matrix spectroscopy and Fourier

https://doi.org/10.5194/egusphere-2024-74
Preprint. Discussion started: 5 February 2024

transform ion cyclotron resonance mass spectrometry analysis, Atmos. Chem. Phys., 20, 2513-2532, http://doi.org/10.5194/acp-20-2513-2020, 2020.

Tang, S., Li, F., Lv, J., Liu, L., Wu, G., Wang, Y., Yu, W., Wang, Y., and Jiang, G.: Unexpected molecular diversity of brown carbon formed by Maillard-like reactions in aqueous aerosols, Chem. Sci., 13, 8401-8411, http://doi.org/10.1039/d2sc02857c, 2022.

van Pinxteren, D., Plewka, A., Hofmann, D., Müller, K., Kramberger, H., Svrcina, B., Bächmann, K., Jaeschke, W., Mertes, S., Collett, J. L., and Herrmann, H.: Schmücke hill cap cloud and valley stations aerosol characterisation during FEBUKO (II): Organic compounds, Atmos. Environ., 39, 4305-4320, http://doi.org/https://doi.org/10.1016/j.atmosenv.2005.02.014, 2005.

Vidovic, K., Lasic Jurkovic, D., Sala, M., Kroflic, A., and Grgic, I.: Nighttime Aqueous-Phase Formation of Nitrocatechols in the Atmospheric Condensed Phase, Environ. Sci. Technol., 52, 9722-9730, http://doi.org/10.1021/acs.est.8b01161, 2018.

Vione, D., Maurino, V., Minero, C., and Ezio, P.: Aqueous Atmospheric Chemistry: Formation of 2,4-Dinitrophenol upon Nitration of 2-Nitrophenol and 4-Nitrophenol in Solution, Environ. Sci. Technol., 39, 7921-7931, http://doi.org/10.1021/es050824m 2005.

Wang, L., Wang, X., Gu, R., Wang, H., Yao, L., Wen, L., Zhu, F., Wang, W., Xue, L., Yang, L., Lu, K., Chen, J., Wang, T., Zhang, Y., and Wang, W.: Observations of fine particulate nitrated phenols in four sites in northern China: concentrations, source apportionment, and secondary formation, Atmos. Chem. Phys., 18, 4349-4359, http://doi.org/10.5194/acp-18-4349-2018, 2018.

Wang, Y., Hu, M., Lin, P., Tan, T., Li, M., Xu, N., Zheng, J., Du, Z., Qin, Y., Wu, Y., Lu, S., Song, Y., Wu, Z., Guo, S., Zeng, L., Huang, X., and He, L.: Enhancement in Particulate Organic Nitrogen and Light Absorption of Humic-Like Substances over Tibetan Plateau Due to Long-Range Transported Biomass Burning Emissions, Environ. Sci. Technol., 53, 14222-14232, http://doi.org/10.1021/acs.est.9b06152, 2019.

Xu, W., Han, T., Du, W., Wang, Q., Chen, C., Zhao, J., Zhang, Y., Li, J., Fu, P., Wang, Z., Worsnop, D. R., and Sun, Y.: Effects of Aqueous-Phase and Photochemical Processing on Secondary Organic Aerosol Formation and Evolution in Beijing, China, Environ. Sci. Technol., 51, 762-770, http://doi.org/10.1021/acs.est.6b04498, 2017.

Yang, L., Huang, R. J., Yuan, W., Huang, D. D., and Huang, C.: pH-Dependent Aqueous-Phase Brown Carbon Formation: Rate Constants and Implications for Solar Absorption and Atmospheric Photochemistry, Environ. Sci. Technol., http://doi.org/10.1021/acs.est.3c07631, 2024.

Yang, L., Huang, R. J., Shen, J., Wang, T., Gong, Y., Yuan, W., Liu, Y., Huang, H., You, Q., Huang, D. D., and Huang, C.: New Insights into the Brown Carbon Chromophores and Formation Pathways for Aqueous Reactions of alpha-Dicarbonyls with Amines and Ammonium, Environ. Sci. Technol., 57, 12351-12361, http://doi.org/10.1021/acs.est.3c04133, 2023.

https://doi.org/10.5194/egusphere-2024-74
Preprint. Discussion started: 5 February 2024

Yang, Z., Tsona, N. T., George, C., and Du, L.: Nitrogen-Containing Compounds Enhance Light Absorption of Aromatic-Derived Brown Carbon, Environ. Sci. Technol., 56, 4005-4016, http://doi.org/10.1021/acs.est.1c08794, 2022.

Zhang, H., Li, R., Dong, S., Wang, F., Zhu, Y., Meng, H., Huang, C., Ren, Y., Wang, X., Hu, X., Li, T., Peng, C., Zhang, G., Xue, L., Wang, X., and Tang, M.: Abundance and Fractional Solubility of Aerosol Iron During Winter at a Coastal City in Northern China: Similarities and Contrasts Between Fine and Coarse Particles, J. Geophys. Res. Atmos., 127, http://doi.org/10.1029/2021jd036070, 2021.